

Characterization and Modeling of Dynamic On-Body Propagation at 4.5 GHz

Bin Zhen, *Member, IEEE*, Minseok Kim, *Member, IEEE*, Jun-ichi Takada, *Member, IEEE*, and Ryuji Kohno

Abstract—On-body communication channels are of increasing interest as more and more wireless devices are wearable in medical, military, and personal communications. This letter presents an experimental investigation into the dynamic on-body channel with body movements. Based on statistical analyses of level crossing rate and fading duration, a three-state Fritchman model that considers both channel dwelling time and channel quality is proposed to describe the burst characteristics of on-body fading. The dynamic on-body channels are classified into unstable error-free state, constant error-free state, and error state. Parameters for the Fritchman model are estimated from the measured data.

Index Terms—Body area networks, channel characterization, finite-state Markov model, on-body propagation.

I. INTRODUCTION

WIRELESS connection between wearable devices is preferred for its ease of usage and the comfort and mobility of users [1]. A significant feature of such an on-body channel is the nonstationary propagation path between two points on the human body. Even when standing still, the human body is subject to small movements, such as from breathing.

On-body propagation channels have been investigated in different frequency bands and environments [2]–[8]. The combination of transmitted signals along a multipath produces a distorted waveform at the receiver. The on-body path loss can be well described by the log-normal distribution. The power-delay profiles can be described based on the well-defined S-V model [9]. Significant channel fading was observed when the whole body or part of the body was in movement [3], [8]. Except for waveform level models mentioned, finite-state Markov chain (FSMC) has successfully modeled the burst error behavior in the flat fading channels in a discrete manner [10], [11]. A generalized Gilbert–Elliott model partitions channel quality into a finite number of intervals, each of which corresponds to one state of the channel [12]–[14]. The simplest Gilbert channel has two states, one with total absence of errors and one with a defined error occurrence probability [12], [13].

This letter focuses on modeling dynamic on-body channels with continuous body movements. Statistics for the burst behaviors of the dynamic channel were first examined. Then, a

Manuscript received August 14, 2009. First published November 17, 2009; current version published December 08, 2009.

B. Zhen and R. Kohno are with the National Institute of Information and Communications Technology, Yokosuka, 239-0847, Japan (e-mail: zhen.bin@nict.go.jp).

M. Kim and J.-i. Takada are with the Tokyo Institute of Technology, Tokyo 152-8550, Japan.

Color versions of one or more of the figures in this letter are available online at <http://ieeexplore.ieee.org>.

Digital Object Identifier 10.1109/LAWP.2009.2036749

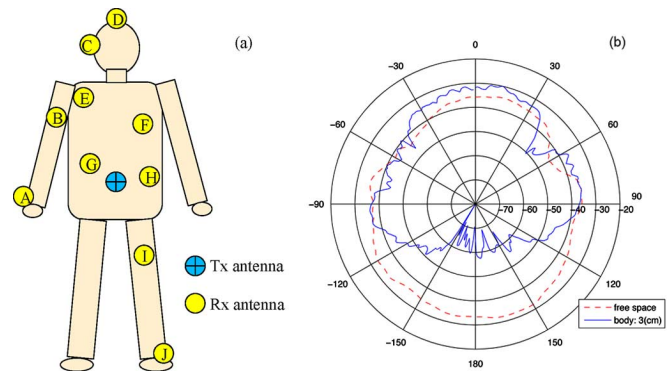


Fig. 1. (a) Measurement locations on the human body, and (b) the radiation pattern of antenna on body surface.

three-state Fritchman model was presented to describe the burst characteristics in a mathematical form.

II. ON-BODY MEASUREMENT SETUP

Dynamic on-body channel measurements were conducted in a radio anechoic chamber where multipath effect from surrounding objects was negligible. The test subject was an adult male in his early 20s whose height, chest, and waist measurements were 171.5, 89.5, and 76.5 cm, respectively. Fig. 1(a) shows the measurement setup. The transmit antenna, Tx, was fixed at a position around the navel, and there were 10 receive antenna, Rx, positions. The antenna used (SkyCross SMT-3TO10M-A) was small meander-line-type antenna that covers a wide frequency range between 3.1 to 10 GHz. The antenna was mounted 3 cm above the body surface by foamed polystyrene. The antennas and RF cable were fastened by a belt to minimize their movements when the subject was in motion.

The dynamic on-body channel was measured by a real-time channel sounder from MEDAV [15]. Single-input–single-output (SISO) measurement mode was used. The test signal was a periodic 193-tone signal with a center frequency of 4.5 GHz and a bandwidth of 120 MHz. Frequency domain channel response was obtained in every 1 ms. Fig. 1(b) shows the radiation pattern of the body surface-attached SkyCross antenna.

Measurements were performed for three scenarios: the reference scenario with the subject standing still and two dynamic scenarios with the subject walking in place and standing up and sitting down on the chair. In each scenario, measurements were conducted one by one at each of the 10 Rx positions. The distances between the Tx antenna and Rx antennas in the reference scenario are given in Table I. Each action was measured for a 10-s session. The subject walked at least eight steps and stood up and down five times during this period. Approximately 10 000

TABLE I
STATISTICAL PARAMETERS FOR THE DYNAMIC ON-BODY CHANNEL ($\theta = -10$ dB)

Positions	Distance (mm)	Walking				Standing up/down			
		Relative path gain (dB)	Level crossing (times)	Average duration (ms)		Relative path gain (dB)	Level crossing (times)	Average duration (ms)	
				Error-free channels	Error channels			Error-free channels	Error channels
A: right wrist	440~525	-3.99±11.77	31	217.03	104.97	8.45±3.48	0	10,000	0
B: right-upper arm	360	4.45±2.50	0	10,000	0	6.30±5.67	16	423.33	11.88
C: right ear	710	-4.15±2.47	60	159.03	1.65	-3.13±5.25	204	37.56	7.15
D: head	650	-3.54±3.21	37	67.64	2.78	-3.69±3.21	123	62.06	10.23
E: shoulder	310	-1.80±2.05	0	10,000	0	0.22±4.10	3	7	1
F: chest	230	3.64±2.47	0	10,000	0	5.08±6.41	17	572.56	14.12
G: right rib	183	-0.89±1.40	0	10,000	0	5.70±3.21	0	10,000	0
H: left waist	140	-1.50±0.98	0	10,000	0	-3.56±3.35	8	1105.25	51.88
I: left thigh	340	-2.69±2.65	9	750.35	1.89	-0.60±3.77	14	710.08	23.43
J: left ankle	815~940	0.94±3.70	18	574.12	10.5	-1.13±4.72	30	262.48	20.17

snapshots of channel response were captured in each measurement session.

III. RESULTS AND ANALYSIS

A. Relative Path Gain

The snapshot of channel response in frequency domain was converted into time domain by a 193-point fast Fourier transform (FFT) operation. The peak value of the channel impulse response was considered as the path gain of the measured instant. For each Rx antenna position in the reference scenario, all path gains in the reference scenario were averaged to obtain a reference path gain. The instant path gain at a position in the two dynamic scenarios was normalized by the reference path gain to obtain the relative path gain in dB. The relative path gain can partially remove the impact of distance between Tx and Rx at different positions.

Channel responses in the frequency domain have shown that fading that result from body movements are non-frequency-selective. Fig. 2 draws time variations of the relative path gain at position A in three scenarios. The on-body channel experienced significant fading that follows the subject motion in a regular base. This is expected as movement causes variations in the separation and orientation of antennas. In some cases, the movement may introduce obstacles between antennas and significantly change the relative path gain. Even in the reference scenario, involuntary movements of the subject may cause irregular and abrupt fading at some instants. Table I shows statistic parameters of the relative path gains at each Rx position.

B. Statistic Analyses

By combining all measurement sessions at 10 antenna positions together, a general concept of on-body fading that is independent of antenna positions and dynamic scenarios was obtained. As shown in Fig. 3, the probability distribution function (PDF) of relative path gains calculated in step of 1 dB was fitted by normal distribution, $N(0.1, 5.4)$, using a maximum likelihood estimate.

Medical sensors usually prefer simple modulations without complex error coding for reasons of complexity, cost, and power

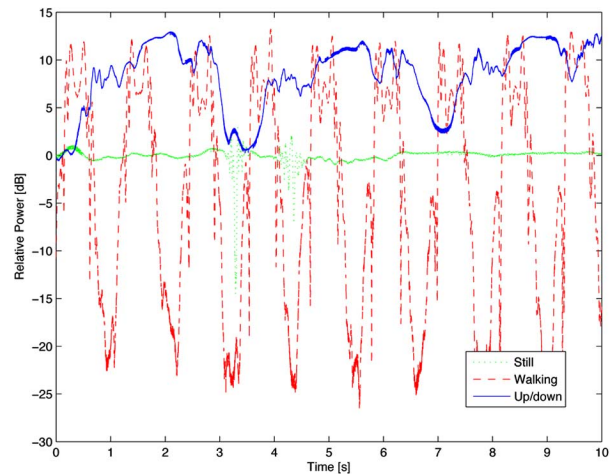


Fig. 2. Relative path gain at position A (right wrist).

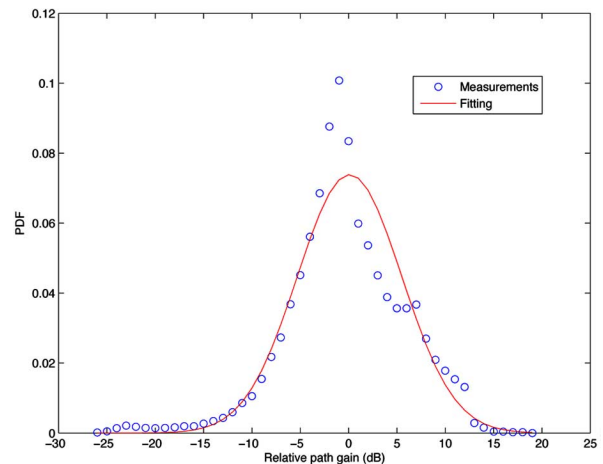


Fig. 3. PDF of relative path gain and its fitting.

consumption. Performance of simple modulations deteriorates severely when the signal quality is lower than a threshold θ . Packet error usually occurs during this period. Fig. 4 plots average level crossing rate (LCR), which is the frequency of a

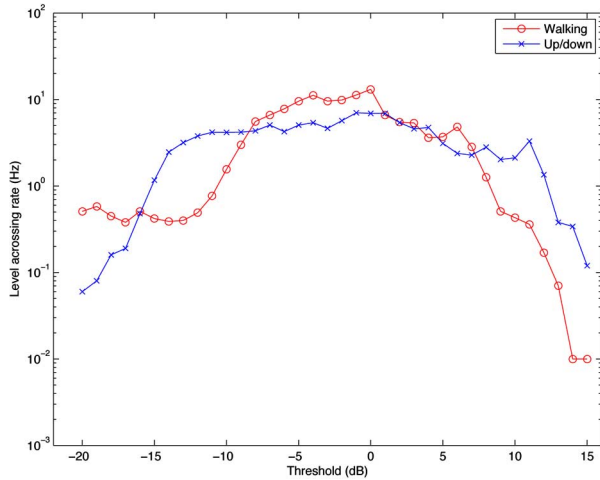


Fig. 4. Average LCR in two dynamic scenarios.

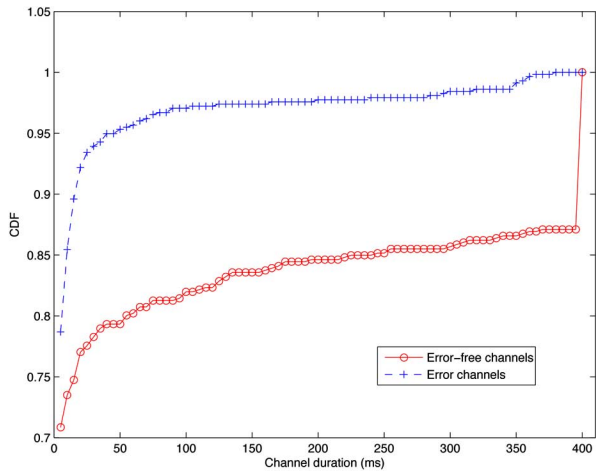


Fig. 5. CDF of durations of error channels and error-free channels in two dynamic scenarios ($\theta = -10$ dB).

signal crossing a threshold in a positive or negative going direction, for two dynamic scenarios. Table I lists total times of level crossing for each action for $\theta = -10$ dB. The value of -10 dB was selected because it was typically the least link margin for a system design. The LCR depends on the mobility of subject and antenna position. It was zero at position A during the standing up/down scenario, while it was zero at position B during the walking scenario. In this letter, we say fading occurs when the relative path gain crosses the threshold in negative direction. The channel is error-free when the relative path gain is above the threshold. Otherwise, it is an error channel.

The cumulative distribution function (CDF) of durations of error channels for $\theta = -10$ dB in two dynamic scenarios was plotted in Fig. 5. Nearly 90% of error channels were shorter than 10 ms. This confirms that the on-body channel is highly sensitive to body movements. A small movement may have a significant impact on the path gain. None of error channels lasted more than 400 ms. The maximum duration of error channels is related to the velocity and pattern of the movement.

Two adjacent error channels are separated by an error-free channel. The CDF of durations of error-free channels was also

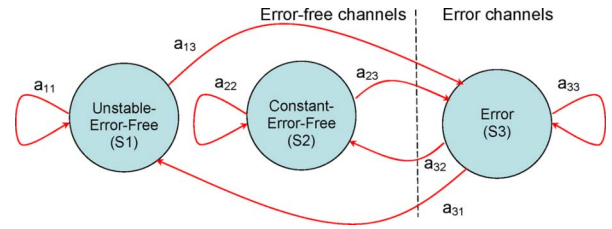


Fig. 6. A three-state Fritchman model for dynamic on-body channels.

drawn in Fig. 5. Although durations of most error-free channels were less than 10 ms, about 13% of error-free channels were longer than 400 ms. In other words, the on-body channel may dwell in the error-free situation for a long time. The ratio of total duration of error channels to that of error-free channels was 4.46%. Table I lists average durations of error channels and error-free channels at each Rx position.

IV. FRITCHMAN CHANNEL MODEL

The Fritchman model was first introduced in 1967 [12]. For binary channels, the Fritchman’s framework divides state space into k error-free states and $N-k$ error states according to link quality, e.g., signal-to-noise ratio (SNR), at receivers [10], [11]. The measured data in Table I and Fig. 5 have shown that the on-body channel dwells in the error-free situation and in the error situation with different patterns. From the viewpoint of medium access control (MAC), the dwelling pattern of channels at different SNRs is important. For example, if an error occurs, retransmission should be arranged until the channel becomes error-free. Fig. 6 shows a three-state Fritchman model that considers both the channel dwelling time and the channel quality. The channel states are defined as:

- S1: unstable error-free state. It is an error-free channel whose duration is shorter than 400 ms.
- S2: constant error-free state. It is an error-free channel whose duration is longer 400 ms. and
- S3: error state. It is an error-free channel.

Error-free channels were further classified into S1 and S2. As shown in Fig. 5, no error channel is longer than 400 ms, and the CDFs of S1 channels and that of S3 channels are similar. We therefore selected 400 ms as a separation point of error-free channels. The state of on-body channels at sample time t is given by

$$\Pi_t = \Pi_{t-1}A \quad t \geq 1, \tag{1}$$

where $A = \begin{bmatrix} a_{11} & 0 & a_{13} \\ 0 & a_{22} & a_{23} \\ a_{31} & a_{32} & a_{33} \end{bmatrix}$ is the state transit matrix and Π_0 is the initial state probability vector. The zero in matrix A means there is no transition between states S1 and S2 because such a transition is indistinguishable from an observed error sequence. The error generation matrix takes a very simple form

$$B = \begin{bmatrix} 1 & 1 & 0 \\ 0 & 0 & 1 \end{bmatrix}. \tag{2}$$

We first classified error channels and error-free channels into different states and then applied the Baum–Welch algorithm to

TABLE II
PARAMETERS OF THE THREE-STATE FRITCHMAN MODEL FOR DIFFERENT THRESHOLDS

Threshold (dB)	A	Π_0
-6	$A = \begin{bmatrix} 0.961 & 0 & 0.0387 \\ 0 & 0.9994 & 0.000590 \\ 0.0454 & 0.00331 & 0.951 \end{bmatrix}$	$\Pi_0 = [0.14 \quad 0.73 \quad 0.12]$
-10	$A = \begin{bmatrix} 0.9536 & 0 & 0.0464 \\ 0 & 0.9996 & 0.000399 \\ 0.056 & 0.0075 & 0.936 \end{bmatrix}$	$\Pi_0 = [0.054 \quad 0.90 \quad 0.044]$
-14	$A = \begin{bmatrix} 0.922 & 0 & 0.0784 \\ 0 & 0.9998 & 0.000183 \\ 0.0612 & 0.00722 & 0.932 \end{bmatrix}$	$\Pi_0 = [0.016 \quad 0.96 \quad 0.02]$

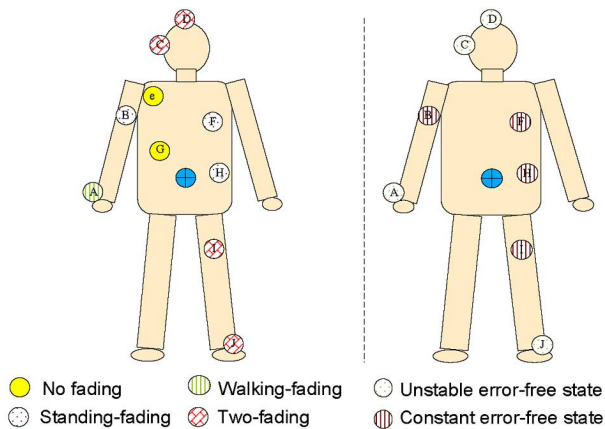


Fig. 7. Map of the on-body fading characteristics.

estimate the parameters in (1) [15]. Table II shows the results for different threshold levels.

It is interesting to map the fading characteristics described by the three-state Fritchman model onto the human body, as shown in Fig. 7. This again confirms that the on-body fading depends on antenna positions and action scenarios. Positions G and E are totally free from fading. Positions A, B, F, and H experience fading during one of the two dynamic scenarios. Other positions experience fading during both dynamic scenarios. The right panel of Fig. 7 classified positions per error-free states. Positions A, C, D, and J experience state S1 during two dynamic scenarios, while other positions always remain in state S2. This can be partially attributed to the fact that all of positions B, F, H, and I are on the body trunk. They therefore underwent relatively small movement variations in amplitude. It is, however, unexpected to see positions C and D that were on the head sustain severe fading, considering that they were relatively static in the considered dynamic scenarios. This might be due to involuntary head movements during actions.

The transit probability from S3 to S1 and S2 is directly related with backoff and retransmission strategy in case of error occurring. Fig. 8 plots average latencies for the first successful retransmission. For packets as short as 1 ms, it is always good to retransmit immediately because an error-free channel with short duration can be used. On the other hand, there is an optimal

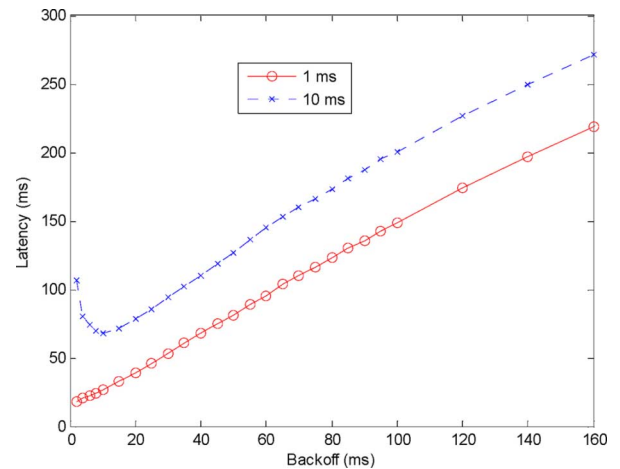


Fig. 8. Latency for the first successful retransmission.

backoff period to achieve minimum latency for a 10-ms-long packet. This is because an immediate retransmission may segment an S1 channel that is just a little longer than the packet duration into two parts. As a result, retransmissions may likely fall outside the error-free period and fail.

V. CONCLUSION

The statistical analyses obtained at 4.5 GHz, such as LCR and fading duration, coincided with research at other frequency bands [3], [4], [6], [8]. This indicates that the dynamic feature of on-body channels is independent of the frequency band.

Typical waveform-level channel models focus on signal strength, multipath, and noise at the receiver [2]–[8]. The result is a sample-by-sample-based data. FSMC-based models provide an abstract of the physical channel with a simple state transit matrix and allow system-level performance evaluation in closed form. They can operate on either a symbol-by-symbol level or a frame-by-frame level. Thus, the simulation time can be greatly reduced. Besides, it is easier to interface with the upper-layer protocols. Traditionally, each FSMC state in the channel model represents a range of received SNR, which in turn determines the error probability of states [10]–[15]. Example criteria include bit or packet error rate, packet error

distribution, and packet throughput [16]. In addition to SNR, the Fritchman model presented takes channel dwelling time into consideration as well. The error-free channel especially should be further classified. This allows optimization of the retransmission once an error occurs.

In this letter, the dynamic characteristics of the on-body channel at 4.5 GHz have been investigated in an anechoic chamber. The channel responses at 10 antenna positions have been obtained for two dynamic scenarios: walking and standing up/sitting down. Statistical analyses of relative path gain, LCR, and fading duration are presented. Based on the statistics, a three-state Fritchman model has been developed to describe the time-varying characteristics. The dynamic on-body channels are classified as unstable error-free state, constant error-free state, and error state according to the dwelling time in different channel qualities. Parameters of the three-state Fritchman model have been estimated.

REFERENCES

- [1] D. Cypher, N. Chevrollier, N. Montavont, and N. Golmie, "Prevailing over wires in healthcare environments: Benefits and challenges," *IEEE Commun. Mag.*, vol. 44, no. 4, pp. 56–63, Apr. 2006.
- [2] K. Y. Yazdandoost, "Channel model for body area networks (BAN)," IEEE 802.15-08-0033-09, 2008.
- [3] P. S. Hall *et al.*, "Antenna and propagation for on-body communication systems," *IEEE Antennas Propag. Mag.*, vol. 49, no. 3, pp. 41–58, Mar. 2007.
- [4] S. L. Cotton and W. G. Scanlon, "Characterization and modeling of the indoor radio channel at 868 MHz for a mobile bodyworn wireless personal area network," *IEEE Antennas Wireless Propag. Lett.*, vol. 6, pp. 51–55, 2007.
- [5] A. Alomainy *et al.*, "UWB on-body radio propagation and system modeling for wireless body-centric networks," *IEE Proc. Commun.*, vol. 153, no. 1, pp. 107–114, 2006.
- [6] Z. H. Hu *et al.*, "Measurements and statistical analysis of on-body channel fading at 2.4 GHz," *IEEE Antennas Wireless Propag. Lett.*, vol. 6, pp. 612–616, 2007.
- [7] J. Ryckaert *et al.*, "Channel model for wireless communication around human body," *Electron. Lett.*, vol. 40, no. 9, pp. 543–544, 2004.
- [8] D. Miniutti *et al.*, "Dynamic narrowband channel measurements around 2.4 GHz for body area networks," IEEE P802.15-08-0354-00-0006, 2008.
- [9] A. Saleh and R. Valenzuela, "A statistical model for indoor multipath propagation," *IEEE J. Sel. Areas Commun.*, vol. 5, no. 2, pp. 128–137, Feb. 1987.
- [10] H. S. Wang and N. Moayeri, "Finite-state Markov channels—A useful model for radio communications channels," *IEEE Trans. Veh. Technol.*, vol. 44, no. 1, pp. 163–171, Feb. 1995.
- [11] J. Garcia-Frias and P. M. Crespo, "Hidden Markov models for burst error characterization in indoor radio channels," *IEEE Trans. Veh. Technol.*, vol. 46, no. 4, pp. 1006–1020, Nov. 1997.
- [12] E. N. Gilbert, "Capacity of burst-noise channel," *Bell Syst. Tech. J.*, vol. 39, pp. 1253–1266, 1960.
- [13] E. O. Elliott, "Estimates of error rates for codes on burst-noise channels," *Bell Syst. Tech. J.*, vol. 42, pp. 1977–1997, 1963.
- [14] B. D. Fritchman, "A binary channel characterization using partitioned Markov chains," *IEEE Trans. Inf. Theory*, vol. IT-13, no. 2, pp. 221–227, Apr. 1967.
- [15] L. E. Baum, T. Petrie, G. Soules, and N. Weiss, "A maximization techniques occurring in the statistical analysis of probability functions of Markov chain," *Ann. Math. Stat.*, vol. 41, no. 1, pp. 164–171, 1970.
- [16] P. Sadeghi, R. A. Kennedy, P. B. Rapajic, and R. Shams, "Finite-state Markov modeling of fading channels," *IEEE Signal Process. Mag.*, vol. 25, no. 5, pp. 57–80, Sep. 2008.